Fermilab FERMILAB-PUB-07-043-E

Search for New Physics in Lepton + Photon + X Events with 929 pb^{-1} of p$\bar{\text{p}}$ Collisions at $\sqrt{s}$= 1.96 TeV

A. Abulencia,[24] J. Adelman,[13] T. Affolder,[10] T. Akimoto,[56] M.G. Albrow,[17] D. Ambrose,[17] S. Amerio,[44] D. Amidei,[35] A. Anastassov,[53] K. Anikeev,[17] A. Annovi,[19] J. Antos,[14] M. Aoki,[56] G. Apollinari,[17] J.-F. Arguin,[34] T. Arisawa,[58] A. Artikov,[15] W. Ashmanskas,[17] A. Attal,[8] F. Azfar,[43] P. Azzi-Bacchetta,[44] P. Azzurri,[47] N. Bacchetta,[44] W. Badgett,[17] A. Barbaro-Galtieri,[29] V.E. Barnes,[49] B.A. Barnett,[25] S. Baroiant,[7] V. Bartsch,[31] G. Bauer,[33] F. Bedeschi,[47] S. Behari,[25] S. Belforte,[55] G. Bellettini,[47] J. Bellinger,[60] A. Belloni,[33] D. Benjamin,[16] A. Beretvas,[17] J. Beringer,[29] T. Berry,[30] A. Bhatti,[51] M. Binkley,[17] D. Bisello,[44] R.E. Blair,[2] C. Blocker,[6] B. Blumenfeld,[25] A. Bocci,[16] A. Bodek,[50] V. Boisvert,[50] G. Bolla,[49] A. Bolshov,[33] D. Bortoletto,[49] J. Boudreau,[48] A. Boveia,[10] B. Brau,[10] L. Brigliadori,[5] C. Bromberg,[36] E. Brubaker,[13] J. Budagov,[15] H.S. Budd,[50] S. Budd,[24] S. Budroni,[47] K. Burkett,[17] G. Busetto,[44] P. Bussey,[21] K. L. Byrum,[2] S. Cabrera^{o},[16] M. Campanelli,[20] M. Campbell,[35] F. Canelli,[17] A. Canepa,[49] S. Carillo^{i},[18] D. Carlsmith,[60] R. Carosi,[47] S. Carron,[34] M. Casarsa,[55] A. Castro,[5] P. Catastini,[47] D. Cauz,[55] M. Cavalli-Sforza,[3] A. Cerri,[29] L. Cerrito^{m},[43] S.H. Chang,[28] Y.C. Chen,[1] M. Chertok,[7] G. Chiarelli,[47] G. Chlachidze,[15] F. Chlebana,[17] I. Cho,[28] K. Cho,[28] D. Chokheli,[15] J.P. Chou,[22] G. Choudalakis,[33] S.H. Chuang,[60] K. Chung,[12] W.H. Chung,[60] Y.S. Chung,[50] M. Ciljak,[47] C.I. Ciobanu,[24] M.A. Ciocci,[47] A. Clark,[20] D. Clark,[6] M. Coca,[16] G. Compostella,[44] M.E. Convery,[51] J. Conway,[7] B. Cooper,[36] K. Copic,[35] M. Cordelli,[19] G. Cortiana,[44] F. Crescioli,[47] C. Cuenca Almenar^{o},[7] J. Cuevas^{l},[11] R. Culbertson,[17] J.C. Cully,[35] D. Cyr,[60] S. DaRonco,[44] M. Datta,[17] S. D'Auria,[21] T. Davies,[21] M. D'Onofrio,[3] D. Dagenhart,[6] P. de Barbaro,[50] S. De Cecco,[52] A. Deisher,[29] G. De Lentdecker^{c},[50] M. Dell'Orso,[47] F. Delli Paoli,[44] L. Demortier,[51] J. Deng,[16] M. Deninno,[5] D. De Pedis,[52] P.F. Derwent,[17] G.P. Di Giovanni,[45] C. Dionisi,[52] B. Di Ruzza,[55] J.R. Dittmann,[4] P. DiTuro,[53] C. Dörr,[26] S. Donati,[47] M. Donega,[20] P. Dong,[8] J. Donini,[44] T. Dorigo,[44] S. Dube,[53] J. Efron,[40] R. Erbacher,[7] D. Errede,[24] S. Errede,[24] R. Eusebi,[17] H.C. Fang,[29] S. Farrington,[30] I. Fedorko,[47] W.T. Fedorko,[13] R.G. Feild,[61] M. Feindt,[26] J.P. Fernandez,[32] R. Field,[18] G. Flanagan,[49] A. Foland,[22] S. Forrester,[7] G.W. Foster,[17] M. Franklin,[22] J.C. Freeman,[29] H. Frisch,[13] I. Furic,[13] M. Gallinaro,[51] J. Galyardt,[12] J.E. Garcia,[47] F. Garberson,[10] A.F. Garfinkel,[49] C. Gay,[61] H. Gerberich,[24] D. Gerdes,[35] S. Giagu,[52] P. Giannetti,[47] A. Gibson,[29] K. Gibson,[48] J.L. Gimmell,[50] C. Ginsburg,[17] N. Giokaris^{a},[15] M. Giordani,[55] P. Giromini,[19] M. Giunta,[47] G. Giurgiu,[12] V. Glagolev,[15] D. Glenzinski,[17] M. Gold,[38] N. Goldschmidt,[18] J. Goldstein^{b},[43] A. Golossanov,[17] G. Gomez,[11] G. Gomez-Ceballos,[11] M. Goncharov,[54] O. González,[32] I. Gorelov,[38] A.T. Goshaw,[16] K. Goulianos,[51] A. Gresele,[44] M. Griffiths,[30] S. Grinstein,[22] C. Grosso-Pilcher,[13] R.C. Group,[18] U. Grundler,[24] J. Guimaraes da Costa,[22] Z. Gunay-Unalan,[36] C. Haber,[29] K. Hahn,[33] S.R. Hahn,[17] E. Halkiadakis,[53] A. Hamilton,[34] B.-Y. Han,[50] J.Y. Han,[50] R. Handler,[60] F. Happacher,[19] K. Hara,[56] M. Hare,[57] S. Harper,[43] R.F. Harr,[59] R.M. Harris,[17] M. Hartz,[48] K. Hatakeyama,[51] J. Hauser,[8] A. Heijboer,[46] B. Heinemann,[30] J. Heinrich,[46] C. Henderson,[33] M. Herndon,[60] J. Heuser,[26] D. Hidas,[16] C.S. Hill^{b},[10] D. Hirschbuehl,[26] A. Hocker,[17] A. Holloway,[22] S. Hou,[1] M. Houlden,[30] S.-C. Hsu,[9] B.T. Huffman,[43] R.E. Hughes,[40] U. Husemann,[61] J. Huston,[36] J. Incandela,[10] G. Introzzi,[47] M. Iori,[52] Y. Ishizawa,[56] A. Ivanov,[7] B. Iyutin,[33] E. James,[17] D. Jang,[53] B. Jayatilaka,[35] D. Jeans,[52] H. Jensen,[17] E.J. Jeon,[28] S. Jindariani,[18] M. Jones,[49] K.K. Joo,[28] S.Y. Jun,[12] J.E. Jung,[28] T.R. Junk,[24] T. Kamon,[54] P.E. Karchin,[59] Y. Kato,[42] Y. Kemp,[26] R. Kephart,[17] U. Kerzel,[26] V. Khotilovich,[54] B. Kilminster,[40] D.H. Kim,[28] H.S. Kim,[28] J.E. Kim,[28] M.J. Kim,[12] S.B. Kim,[28] S.H. Kim,[56] Y.K. Kim,[13] N. Kimura,[56] L. Kirsch,[6] S. Klimenko,[18] M. Klute,[33] B. Knuteson,[33] B.R. Ko,[16] K. Kondo,[58] D.J. Kong,[28] J. Konigsberg,[18] A. Korytov,[18] A.V. Kotwal,[16] A. Kovalev,[46] A.C. Kraan,[46] J. Kraus,[24] I. Kravchenko,[33] M. Kreps,[26] J. Kroll,[46] N. Krumnack,[4] M. Kruse,[16] V. Krutelyov,[10] T. Kubo,[56] S. E. Kuhlmann,[2] T. Kuhr,[26] Y. Kusakabe,[58] S. Kwang,[13] A.T. Laasanen,[49] S. Lai,[34] S. Lami,[47] S. Lammel,[17] M. Lancaster,[31] R.L. Lander,[7] K. Lannon,[40] A. Lath,[53] G. Latino,[47] I. Lazzizzera,[44] T. LeCompte,[2] J. Lee,[50] J. Lee,[28] Y.J. Lee,[28] S.W. Lee^{n},[54] R. Lefèvre,[3] N. Leonardo,[33] S. Leone,[47] S. Levy,[13] J.D. Lewis,[17] C. Lin,[61] C.S. Lin,[17] M. Lindgren,[17] E. Lipeles,[9] A. Lister,[7] D.O. Litvintsev,[17] T. Liu,[17] N.S. Lockyer,[46] A. Loginov,[61] M. Loreti,[44] P. Loverre,[52] R.-S. Lu,[1] D. Lucchesi,[44] P. Lujan,[29] P. Lukens,[17] G. Lungu,[18] L. Lyons,[43] J. Lys,[29] R. Lysak,[14] E. Lytken,[49] P. Mack,[26] D. MacQueen,[34] R. Madrak,[17] K. Maeshima,[17] K. Makhoul,[33] T. Maki,[23] P. Maksimovic,[25] S. Malde,[43] G. Manca,[30] F. Margaroli,[5] R. Marginean,[17] C. Marino,[26] C.P. Marino,[24] A. Martin,[61] M. Martin,[25] V. Martin^{g},[21] M. Martínez,[3] T. Maruyama,[56] P. Mastrandrea,[52] T. Masubuchi,[56] H. Matsunaga,[56] M.E. Mattson,[59] R. Mazini,[34] P. Mazzanti,[5] K.S. McFarland,[50] P. McIntyre,[54] R. McNulty^{f},[30] A. Mehta,[30] P. Mehtala,[23] S. Menzemer^{h},[11] A. Menzione,[47] P. Merkel,[49] C. Mesropian,[51] A. Messina,[36] T. Miao,[17] N. Miladinovic,[6] J. Miles,[33] R. Miller,[36] C. Mills,[10] M. Milnik,[26] A. Mitra,[1] G. Mitselmakher,[18] A. Miyamoto,[27] S. Moed,[20] N. Moggi,[5] B. Mohr,[8]

R. Moore,[17] M. Morello,[47] P. Movilla Fernandez,[29] J. Mülmenstädt,[29] A. Mukherjee,[17] Th. Muller,[26] R. Mumford,[25] P. Murat,[17] J. Nachtman,[17] A. Nagano,[56] J. Naganoma,[58] I. Nakano,[41] A. Napier,[57] V. Necula,[18] C. Neu,[46] M.S. Neubauer,[9] J. Nielsen,[29] T. Nigmanov,[48] L. Nodulman,[2] O. Norniella,[3] E. Nurse,[31] S.H. Oh,[16] Y.D. Oh,[28] I. Oksuzian,[18] T. Okusawa,[42] R. Oldeman,[30] R. Orava,[23] K. Osterberg,[23] C. Pagliarone,[47] E. Palencia,[11] V. Papadimitriou,[17] A.A. Paramonov,[13] B. Parks,[40] S. Pashapour,[34] J. Patrick,[17] G. Pauletta,[55] M. Paulini,[12] C. Paus,[33] D.E. Pellett,[7] A. Penzo,[55] T.J. Phillips,[16] G. Piacentino,[47] J. Piedra,[45] L. Pinera,[18] K. Pitts,[24] C. Plager,[8] L. Pondrom,[60] X. Portell,[3] O. Poukhov,[15] N. Pounder,[43] F. Prakoshyn,[15] A. Pronko,[17] J. Proudfoot,[2] F. Ptohos[e],[19] G. Punzi,[47] J. Pursley,[25] J. Rademacker[b],[43] A. Rahaman,[48] N. Ranjan,[49] S. Rappoccio,[22] B. Reisert,[17] V. Rekovic,[38] P. Renton,[43] M. Rescigno,[52] S. Richter,[26] F. Rimondi,[5] L. Ristori,[47] A. Robson,[21] T. Rodrigo,[11] E. Rogers,[24] S. Rolli,[57] R. Roser,[17] M. Rossi,[55] R. Rossin,[18] A. Ruiz,[11] J. Russ,[12] V. Rusu,[13] H. Saarikko,[23] S. Sabik,[34] A. Safonov,[54] W.K. Sakumoto,[50] G. Salamanna,[52] O. Saltó,[3] D. Saltzberg,[8] C. Sánchez,[3] L. Santi,[55] S. Sarkar,[52] L. Sartori,[47] K. Sato,[17] P. Savard,[34] A. Savoy-Navarro,[45] T. Scheidle,[26] P. Schlabach,[17] E.E. Schmidt,[17] M.P. Schmidt,[61] M. Schmitt,[39] T. Schwarz,[7] L. Scodellaro,[11] A.L. Scott,[10] A. Scribano,[47] F. Scuri,[47] A. Sedov,[49] S. Seidel,[38] Y. Seiya,[42] A. Semenov,[15] L. Sexton-Kennedy,[17] A. Sfyrla,[20] M.D. Shapiro,[29] T. Shears,[30] P.F. Shepard,[48] D. Sherman,[22] M. Shimojima[k],[56] M. Shochet,[13] Y. Shon,[60] I. Shreyber,[37] A. Sidoti,[47] P. Sinervo,[34] A. Sisakyan,[15] J. Sjolin,[43] A.J. Slaughter,[17] J. Slaunwhite,[40] K. Sliwa,[57] J.R. Smith,[7] F.D. Snider,[17] R. Snihur,[34] M. Soderberg,[35] A. Soha,[7] S. Somalwar,[53] V. Sorin,[36] J. Spalding,[17] F. Spinella,[47] T. Spreitzer,[34] P. Squillacioti,[47] M. Stanitzki,[61] A. Staveris-Polykalas,[47] R. St. Denis,[21] B. Stelzer,[8] O. Stelzer-Chilton,[43] D. Stentz,[39] J. Strologas,[38] D. Stuart,[10] J.S. Suh,[28] A. Sukhanov,[18] H. Sun,[57] T. Suzuki,[56] A. Taffard,[24] R. Takashima,[41] Y. Takeuchi,[56] K. Takikawa,[56] M. Tanaka,[2] R. Tanaka,[41] M. Tecchio,[35] P.K. Teng,[1] K. Terashi,[51] J. Thom[d],[17] A.S. Thompson,[21] E. Thomson,[46] P. Tipton,[61] V. Tiwari,[12] S. Tkaczyk,[17] D. Toback,[54] S. Tokar,[14] K. Tollefson,[36] T. Tomura,[56] D. Tonelli,[47] S. Torre,[19] D. Torretta,[17] S. Tourneur,[45] W. Trischuk,[34] R. Tsuchiya,[58] S. Tsuno,[41] N. Turini,[47] F. Ukegawa,[56] T. Unverhau,[21] S. Uozumi,[56] D. Usynin,[46] S. Vallecorsa,[20] N. van Remortel,[23] A. Varganov,[35] E. Vataga,[38] F. Vázquez[i],[18] G. Velev,[17] G. Veramendi,[24] V. Veszpremi,[49] R. Vidal,[17] I. Vila,[11] R. Vilar,[11] T. Vine,[31] I. Vollrath,[34] I. Volobouev[n],[29] G. Volpi,[47] F. Würthwein,[9] P. Wagner,[54] R.G. Wagner,[2] R.L. Wagner,[17] J. Wagner,[26] W. Wagner,[26] R. Wallny,[8] S.M. Wang,[1] A. Warburton,[34] S. Waschke,[21] D. Waters,[31] M. Weinberger,[54] W.C. Wester III,[17] B. Whitehouse,[57] D. Whiteson,[46] A.B. Wicklund,[2] E. Wicklund,[17] G. Williams,[34] H.H. Williams,[46] P. Wilson,[17] B.L. Winer,[40] P. Wittich[d],[17] S. Wolbers,[17] C. Wolfe,[13] T. Wright,[35] X. Wu,[20] S.M. Wynne,[30] A. Yagil,[17] K. Yamamoto,[42] J. Yamaoka,[53] T. Yamashita,[41] C. Yang,[61] U.K. Yang[j],[13] Y.C. Yang,[28] W.M. Yao,[29] G.P. Yeh,[17] J. Yoh,[17] K. Yorita,[13] T. Yoshida,[42] G.B. Yu,[50] I. Yu,[28] S.S. Yu,[17] J.C. Yun,[17] L. Zanello,[52] A. Zanetti,[55] I. Zaw,[22] X. Zhang,[24] J. Zhou,[53] and S. Zucchelli[5]

(CDF Collaboration*)

[1] *Institute of Physics, Academia Sinica, Taipei, Taiwan 11529, Republic of China*
[2] *Argonne National Laboratory, Argonne, Illinois 60439*
[3] *Institut de Fisica d'Altes Energies, Universitat Autonoma de Barcelona, E-08193, Bellaterra (Barcelona), Spain*
[4] *Baylor University, Waco, Texas 76798*
[5] *Istituto Nazionale di Fisica Nucleare, University of Bologna, I-40127 Bologna, Italy*
[6] *Brandeis University, Waltham, Massachusetts 02254*
[7] *University of California, Davis, Davis, California 95616*
[8] *University of California, Los Angeles, Los Angeles, California 90024*
[9] *University of California, San Diego, La Jolla, California 92093*
[10] *University of California, Santa Barbara, Santa Barbara, California 93106*
[11] *Instituto de Fisica de Cantabria, CSIC-University of Cantabria, 39005 Santander, Spain*
[12] *Carnegie Mellon University, Pittsburgh, PA 15213*
[13] *Enrico Fermi Institute, University of Chicago, Chicago, Illinois 60637*
[14] *Comenius University, 842 48 Bratislava, Slovakia; Institute of Experimental Physics, 040 01 Kosice, Slovakia*
[15] *Joint Institute for Nuclear Research, RU-141980 Dubna, Russia*
[16] *Duke University, Durham, North Carolina 27708*
[17] *Fermi National Accelerator Laboratory, Batavia, Illinois 60510*
[18] *University of Florida, Gainesville, Florida 32611*
[19] *Laboratori Nazionali di Frascati, Istituto Nazionale di Fisica Nucleare, I-00044 Frascati, Italy*
[20] *University of Geneva, CH-1211 Geneva 4, Switzerland*
[21] *Glasgow University, Glasgow G12 8QQ, United Kingdom*
[22] *Harvard University, Cambridge, Massachusetts 02138*
[23] *Division of High Energy Physics, Department of Physics, University of Helsinki and Helsinki Institute of Physics, FIN-00014, Helsinki, Finland*
[24] *University of Illinois, Urbana, Illinois 61801*

[25]*The Johns Hopkins University, Baltimore, Maryland 21218*
[26]*Institut für Experimentelle Kernphysik, Universität Karlsruhe, 76128 Karlsruhe, Germany*
[27]*High Energy Accelerator Research Organization (KEK), Tsukuba, Ibaraki 305, Japan*
[28]*Center for High Energy Physics: Kyungpook National University, Taegu 702-701, Korea; Seoul National University, Seoul 151-742, Korea; and SungKyunKwan University, Suwon 440-746, Korea*
[29]*Ernest Orlando Lawrence Berkeley National Laboratory, Berkeley, California 94720*
[30]*University of Liverpool, Liverpool L69 7ZE, United Kingdom*
[31]*University College London, London WC1E 6BT, United Kingdom*
[32]*Centro de Investigaciones Energeticas Medioambientales y Tecnologicas, E-28040 Madrid, Spain*
[33]*Massachusetts Institute of Technology, Cambridge, Massachusetts 02139*
[34]*Institute of Particle Physics: McGill University, Montréal, Canada H3A 2T8; and University of Toronto, Toronto, Canada M5S 1A7*
[35]*University of Michigan, Ann Arbor, Michigan 48109*
[36]*Michigan State University, East Lansing, Michigan 48824*
[37]*Institution for Theoretical and Experimental Physics, ITEP, Moscow 117259, Russia*
[38]*University of New Mexico, Albuquerque, New Mexico 87131*
[39]*Northwestern University, Evanston, Illinois 60208*
[40]*The Ohio State University, Columbus, Ohio 43210*
[41]*Okayama University, Okayama 700-8530, Japan*
[42]*Osaka City University, Osaka 588, Japan*
[43]*University of Oxford, Oxford OX1 3RH, United Kingdom*
[44]*University of Padova, Istituto Nazionale di Fisica Nucleare, Sezione di Padova-Trento, I-35131 Padova, Italy*
[45]*LPNHE, Universite Pierre et Marie Curie/IN2P3-CNRS, UMR7585, Paris, F-75252 France*
[46]*University of Pennsylvania, Philadelphia, Pennsylvania 19104*
[47]*Istituto Nazionale di Fisica Nucleare Pisa, Universities of Pisa, Siena and Scuola Normale Superiore, I-56127 Pisa, Italy*
[48]*University of Pittsburgh, Pittsburgh, Pennsylvania 15260*
[49]*Purdue University, West Lafayette, Indiana 47907*
[50]*University of Rochester, Rochester, New York 14627*
[51]*The Rockefeller University, New York, New York 10021*
[52]*Istituto Nazionale di Fisica Nucleare, Sezione di Roma 1, University of Rome "La Sapienza," I-00185 Roma, Italy*
[53]*Rutgers University, Piscataway, New Jersey 08855*
[54]*Texas A&M University, College Station, Texas 77843*
[55]*Istituto Nazionale di Fisica Nucleare, University of Trieste/ Udine, Italy*
[56]*University of Tsukuba, Tsukuba, Ibaraki 305, Japan*
[57]*Tufts University, Medford, Massachusetts 02155*
[58]*Waseda University, Tokyo 169, Japan*
[59]*Wayne State University, Detroit, Michigan 48201*
[60]*University of Wisconsin, Madison, Wisconsin 53706*
[61]*Yale University, New Haven, Connecticut 06520*

(Dated: February 16, 2007)

We present results of a search at CDF in 929 ± 56 pb^{-1} of $p\bar{p}$ collisions at 1.96 TeV for the anomalous production of events containing a high-transverse momentum charged lepton (ℓ, either e or μ) and photon (γ), accompanied by missing transverse energy ($\not\!\!E_T$), and/or additional leptons and photons, and jets (X). We use the same selection criteria as in a previous CDF Run I search, but with an order-magnitude larger data set, a higher $p\bar{p}$ collision energy, and the CDF II detector. We find 163 $\ell\gamma\not\!\!E_T + X$ events, compared to an expectation of 150.6 ± 13.0 events. We observe 74 $\ell\ell\gamma + X$ events, compared to an expectation of 65.1 ± 7.7 events. We find no events similar to the Run I $ee\gamma\gamma\not\!\!E_T$ event.

PACS numbers: 13.85.Rm, 12.60.Jv, 13.85.Qk, 14.80.Ly

*With visitors from [a]University of Athens, [b]University of Bristol, [c]University Libre de Bruxelles, [d]Cornell University, [e]University of Cyprus, [f]University of Dublin, [g]University of Edinburgh, [h]University of Heidelberg, [i]Universidad Iberoamericana, [j]University of Manchester, [k]Nagasaki Institute of Applied Science, [l]University de Oviedo, [m]University of London, Queen Mary and Westfield College, [n]Texas Tech University, [o]IFIC(CSIC-Universitat de Valencia),

I. INTRODUCTION

An important test of the standard model (SM) of particle physics [1] is to measure and understand the properties of the highest momentum-transfer particle collisions, which correspond to measurements at the shortest distances. The chief predictions of the SM for these collisions are the numbers and types of the fundamental fermions and gauge bosons that are produced, and their associated kinematic distributions. The predicted high energy behavior of the SM, however, becomes unphysical at an interaction energy on the order of several TeV. New physical phenomena are required to ameliorate this high-energy behavior. These unknown phenomena may involve new elementary particles, new fundamental forces, and/or a modification of space-time geometry. These new phenomena are likely to show up as an anomalous production rate of a combination of the known fundamental particles, including those detector-based signatures such as missing transverse energy ($\not\!\!E_T$) or penetrating particle tracks that within the confines of the SM are associated with neutrinos and muons, respectively.

The unknown nature of possible new phenomena in the energy range accessible at the Tevatron is the motivation for a search strategy that does not focus on a single model or class of models of new physics, but presents a wide net for new phenomena. In this paper we present the results of a comparison of standard model predictions with the rates measured at the Tevatron with the CDF detector for final states containing at least one high-p_T lepton (e or μ) and photon, plus other detected objects (leptons, photons, jets, $\not\!\!E_T$).

The initial motivation for such an inclusive search ("signature-based search") came from the observation in 1995 by the CDF experiment [2] of an event consistent with the production of two energetic photons, two energetic electrons, and large missing transverse energy $\not\!\!E_T$ [3]. This signature is predicted to be very rare in the SM, with the dominant contribution being from the production of four gauge bosons: two W bosons and two photons. The event raised theoretical interest, however, as it had, in addition to large missing transverse momentum, very high total transverse energy, and a pattern of widely-separated leptons and photons that was consistent with the decay of a pair of new heavy particles.

There are many models of new physics that could produce such a signature [4]. Gauge-mediated models of supersymmetry [5], in which the lightest super-partner (LSP) is a light gravitino, provide a model in which each partner of a pair of supersymmetric particles produced in a $p\bar{p}$ interaction decays in a chain that leads to a produced gravitino, visible as $\not\!\!E_T$. If the next-to-lightest neutralino (NLSP) has a photino component, each chain also can result in a photon. Models of supersymmetry in which the symmetry breaking is due to gravity also can produce decay chains with photons [6]. For example, if the NLSP is largely photino-like, and the lightest is largely higgsino, decays of the former to the latter will involve the emission of a photon [7]. More generally, pair-production of selectrons or gauginos can result in final-states with large $\not\!\!E_T$, two photons and two leptons. Models with additional space dimensions [8] predict excited states of the known standard model particles. The production of a pair of excited electrons [9] would provide a natural source for two photons and two electrons (although not $\not\!\!E_T$ unless the pair were produced with some other, undetected, particle.). As in the case of supersymmetry, there are many parameters in such models, with a resulting broad range of possible signatures with multiple gauge bosons [10].

Rather than search the huge parameter space of the models current at that time, the CDF Run I analyses that followed up on the $ee\gamma\gamma\not\!\!E_T$ event used a strategy of "signature-based" inclusive searches to cast a wider net for new phenomena: in this case one search for two photons + X ($\gamma\gamma + X$) [2], and a second for one lepton + one photon + X ($\ell\gamma + X$) [11–13], where X can be e, μ, γ, or $\not\!\!E_T$, plus any number of jets. In particular the latter signature, the subject of this present paper, would be sensitive to decay chains in which only one chain produces a photon, a broader set of models.

The Run I $\ell\gamma + X$ search found good agreement with SM predictions in 86 pb^{-1} of data at a center-of-mass energy of 1.8 TeV, except in the $\ell\gamma\not\!\!E_T$ channel, in which 16 events were observed with an expectation of 7.6 $\pm$ 0.7, corresponding to a 2.7σ excess. The Run I paper concluded: "However, an excess of events with 0.7% likelihood (equivalent to 2.7 standard deviations for a Gaussian distribution) in one subsample among the five studied is an interesting result, but it is not a compelling observation of new physics. We look forward to more data in the upcoming run of the Fermilab Tevatron." [12].

Here we present the results from Run II with more than 10 times the statistics of the Run I measurement. We have repeated the $\ell\gamma + X$ search with the same kinematic selection criteria in a data set corresponding to an exposure of 929 ± 56 pb^{-1}, a higher $p\bar{p}$ collision energy, 1.96 TeV, and the CDF II detector [14]. The results correspond to the full data set taken during the period March, 2002 through February, 2006, and include data from the first third of this sample which have already been presented [15]. We give a detailed description of the selection criteria, background calculations, and kinematic distributions for the $\ell\gamma\not\!\!E_T$ and $\ell\ell\gamma$ channels. We also present results for the first time for the $e\mu\gamma + X$ and $\ell\gamma\gamma$ signatures.

This paper is organized as follows. Section II gives a brief description of the CDF II detector, emphasizing the changes from Run I. Section III presents the electron, muon, photon, and $\not\!\!E_T$ identification criteria, and the kinematic event selection criteria. The data flow as additional selection criteria are added, resulting in the measured number of events in each signature, is also described. The standard model W and Z samples, used as control samples, are described in Section IV. Sec-

tion V gives an introduction to the selection of the Inclusive $\ell\gamma + X$ event sample. Section VI describes the selection of the $\ell\gamma \not\!\!E_T$ signal sample, and presents the measured kinematic distributions. Similarly, the $\ell\ell\gamma$ signal sample selection and kinematic distributions are presented in Section VII. A search for the $\ell\gamma\gamma$ signature is briefly described in Section VIII. Section IX summarizes the SM expectations from $W\gamma, W\gamma\gamma, Z\gamma, Z\gamma\gamma$ production, and backgrounds from misidentified photons, $\not\!\!E_T$, and/or leptons. Sections X and XI summarize the results and present the conclusions, respectively.

II. THE CDF II DETECTOR

The CDF II detector is a cylindrically symmetric spectrometer designed to study $p\bar{p}$ collisions at the Fermilab Tevatron based on the same solenoidal magnet and central calorimeters as the CDF I detector [16]. Because the analysis described here is intended to repeat the Run I search as closely as possible, we note especially the differences from the CDF I detector relevant to the detection of leptons, photons, and $\not\!\!E_T$. The tracking systems used to measure the momenta of charged particles have been replaced with a central outer tracker (COT) with smaller drift cells [17], and an enhanced system of silicon strip detectors [18]. The calorimeters in the regions [19] with pseudorapidity $|\eta| > 1$ have been replaced with a more compact scintillator-based design, retaining the projective geometry [20]. The coverage in φ of the central upgrade muon detector (CMP) and central extension muon detector (CMX) systems [21] has been extended; the central muon detector (CMU) system is unchanged.

III. SELECTION OF $\ell\gamma + X$ EVENTS

In order to make the present search statistically *a priori*, the identification of leptons and photons is essentially the same as in the Run I search [11], with only minor technical changes due to the differences in detector details between the upgraded CDF II detector and CDF I.

The scope and strategy of the Run I analysis were designed to reflect the motivating principles. Categories of photon-lepton events were defined *a priori* in a way that characterized the different possibilities for new physics. For each category, the inclusive event total and basic kinematic distributions can be compared with standard model expectations. The decay products of massive particles are typically isolated from other particles, and possess large transverse momentum and low rapidity. The search is therefore limited to those events with at least one isolated, central ($|\eta| < 1.0$) photon with $E_T > 25$ GeV, and at least one isolated, central electron or muon with $E_T > 25$ GeV. These photon-lepton candidates are further partitioned by angular separation. Events where exactly one photon and one lepton are detected nearly opposite in azimuth ($\Delta\varphi_{\ell\gamma} > 150^\circ$) are characteristic of a two-particle final-state (two-body photon-lepton events), and the remaining photon-lepton events are characteristic of three or more particles in the final-state (multi-body photon-lepton events). The multi-body photon-lepton events are then further studied for the presence of additional particles: photons, leptons, or the missing transverse energy associated with weakly interacting neutral particles.

In the subsections below we describe the real-time ("online") event selection criteria by the trigger system, and the subsequent event selection "offline", including the selection of electrons, muons, and photons, the rejection of jet background for leptons and photons by track and calorimeter "isolation" requirements, and the construction of the missing transverse energy $\not\!\!E_T$ and total transverse energy H_T.

A. The Online Selection by the Trigger System

A 3-level trigger system [14] selects events with a high transverse momentum (p_T) [3] lepton ($p_T > 18$ GeV) or photon ($E_T > 25$ GeV) in the central region, $|\eta| \lesssim 1.0$. The trigger system selects photon and electron candidates from clusters of energy in the central electromagnetic calorimeter. Electrons are distinguished from photons by the presence of a COT track pointing at the cluster. The muon trigger requires a COT track that extrapolates to a track segment ("stub") in the muon chambers [22]. At each trigger level all transverse momenta are calculated using the nominal center of the interaction region along the beam-line, $z = 0$ [19].

B. Overview of Event Selection

Inclusive $\ell\gamma$ events (Fig. 1) are selected by requiring a central γ candidate with $\mathrm{E}_\mathrm{T}^\gamma > 25$ GeV and a central e or μ with $\mathrm{E}_\mathrm{T}^\ell > 25$ GeV originating less than 60 cm along the beam-line from the detector center and passing the "tight" criteria listed below. All transverse momenta, including that of the photon, are calculated using the vertex within ± 5 cm of the lepton origin that has the largest scalar sum of transverse momentum from tracks associated to that vertex. Both signal and control samples are drawn from this $\ell\gamma$ sample (Fig. 1).

Considering the control samples first, from the $\ell\gamma$ sample we select back-to-back events with exactly one photon and one lepton (i.e. $\not\!\!E_T < 25$ GeV); this is the dominant contribution to the $\ell\gamma$ sample, and has a large Drell-Yan component. A subset of this sample is the 'Z-like' sample, which provides the calibration for the probability that an electron radiates and is detected as a photon, as discussed in Section IX B 1. The remaining back-to-back events are called the Two-Body Events and were not used in this analysis.

All events which either have more than one lepton or photon, or in which the lepton and photon are not back-to-back (and hence the event cannot be a Two-Body event), are classified as 'Inclusive Multi-Body $\ell\gamma + X$'. These are further subdivided into three categories: $\ell\gamma\not\!\!E_T$ (Section V) ('Multi-Body $\ell\gamma\not\!\!E_T$ Events'), for which the $\not\!\!E_T$ (Section III B 5) is greater than 25 GeV , $\ell\ell\gamma$ (Section VII) and $\ell\gamma\gamma$ (Section VIII) ('Multi-Photon and Multi-Lepton Events'), and events with exactly one lepton and exactly one photon, which are not back-to-back. The events with exactly one lepton and exactly one photon, which are not back-to-back were not used in the analysis.

1. Electron Selection

An electron candidate passing the "tight" selection must have: a) a high-quality track in the COT with $p_T > 0.5\ E_T$, unless $E_T > 100$ GeV, in which case the p_T threshold is set to 25 GeV; b) a good transverse shower profile at shower maximum [23] that matches the extrapolated track position; c) a lateral sharing of energy in the two calorimeter towers containing the electron shower consistent with that expected; and d) minimal leakage into the hadron calorimeter [24].

Additional central electrons are required to have $E_T >$ 20 GeV and to satisfy the tight central electron criteria but with a track requirement of only $p_T > 10$ GeV (rather than $0.5\times E_T$), and no requirement on a shower maximum measurement or lateral energy sharing between calorimeter towers. Electrons in the end-plug calorimeters ($1.2 < |\eta| < 2.0$) are required to have $E_T > 15$ GeV, minimal leakage into the hadron calorimeter, a "track" containing at least 3 hits in the silicon tracking system, and a shower transverse shape consistent with that expected, with a centroid close to the extrapolated position of the track [25].

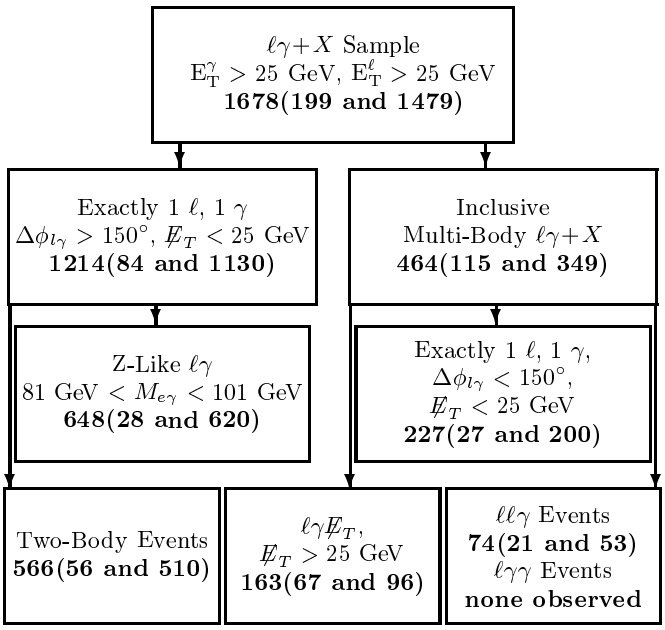

FIG. 1: $\ell\gamma+X$ Sample: the subsets of inclusive lepton-photon events analyzed. The number of events in each subcategory is given as a sum of muons and electrons. The first term in parethesis refers to $\mu\gamma+X$ while the latter refers to the $e\gamma+X$.

2. Muon Selection

A muon candidate passing the "tight" cuts must have: a) a well-measured track in the COT with $p_T > 25$ GeV; b) energy deposited in the calorimeter consistent with expectations [26]; c) a muon "stub" [22] in both the CMU and CMP, or in the CMX, consistent with the extrapolated COT track [27]; and d) COT timing consistent with a track from a $p\bar{p}$ collision [28].

Additional muons are required to have $p_T > 20$ GeV and to satisfy the same criteria as for "tight" muons but with fewer hits required on the track, or, alternatively, for muons outside the muon system fiducial volume, a more stringent cut on track quality but no requirement that there be a matching "stub" in the muon systems [29].

3. Photon Selection

Photon candidates are required to have: no associated track with $p_T > 1$ GeV; at most one track with $p_T < 1$ GeV, pointing at the calorimeter cluster; good profiles in both transverse dimensions at shower maximum; and minimal leakage into the hadron calorimeter [24].

4. 'Isolated' Leptons and Photons

To reduce background from photons or leptons from the decays of hadrons produced in jets, both the photon and the lepton in each event are required to be "isolated" [30]. The E_T deposited in the calorimeter towers in a cone in $\eta - \varphi$ space [19] of radius $R = 0.4$ around the photon or lepton position is summed, and the E_T due to the photon or lepton is subtracted. The remaining E_T is required to be less than 2.0 GeV $+ 0.02 \times (E_T - 20$ GeV) for a photon, or less than 10% of the E_T for electrons or p_T for muons. In addition, for photons the scalar sum of the p_T of all tracks in the cone must be less than 2.0 GeV $+ 0.005 \times E_T$.

5. Missing Transverse Energy and H_T

Missing transverse energy $\not\!\!E_T$ is calculated from the calorimeter tower energies in the region $|\eta| < 3.6$. Corrections are then made to the $\not\!\!E_T$ for non-uniform calorime-

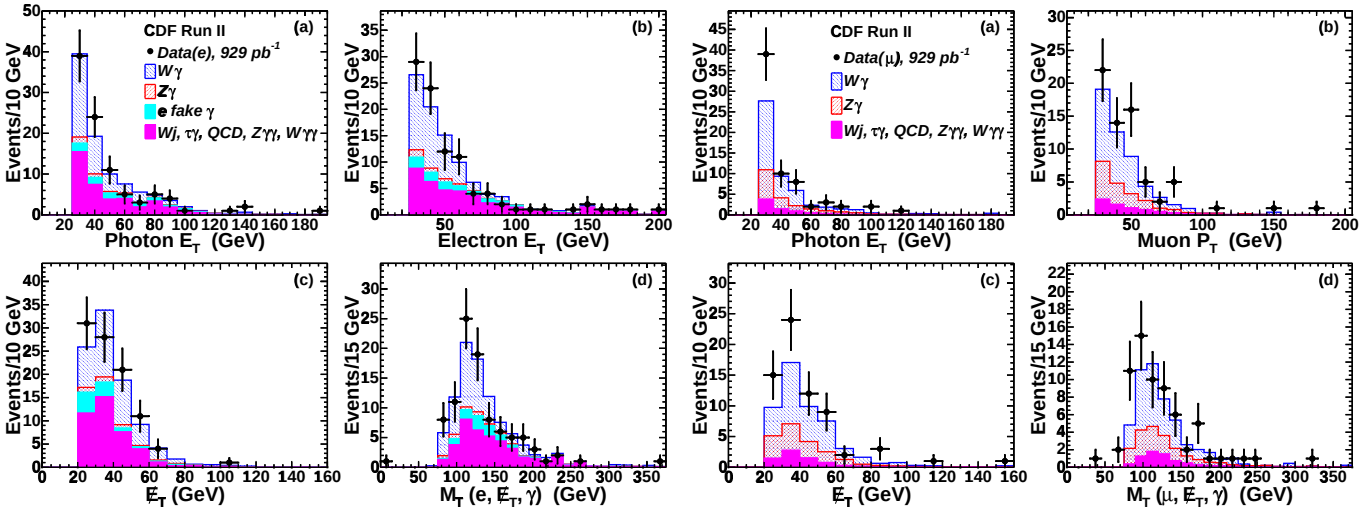

FIG. 2: The distributions for events in the $e\gamma\not\!\!E_T$ sample (points in the left-hand four plots) and the $\mu\gamma\not\!\!E_T$ sample (points in the right-hand four plots) for a) the E_T of the photon; b) the E_T of the lepton; c) the missing transverse energy, $\not\!\!E_T$; and d) the transverse mass of the $\ell\gamma\not\!\!E_T$ system. The histograms show the expected SM contributions, including estimated backgrounds from misidentified photons and leptons.

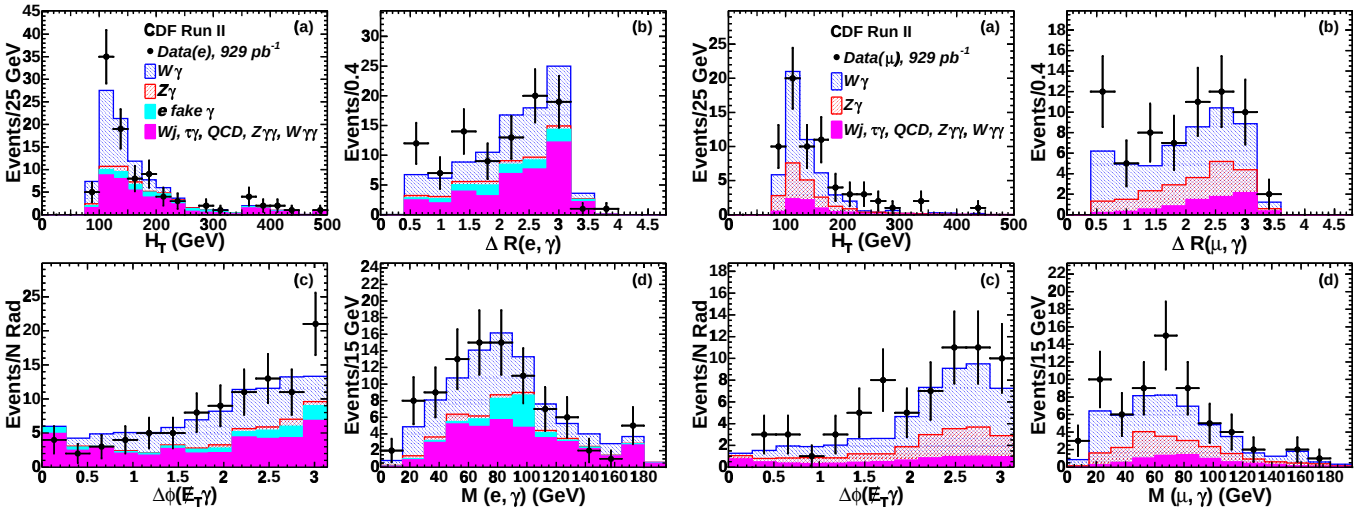

FIG. 3: The distributions for events in the $e\gamma\not\!\!E_T$ sample (points in the left-hand four plots) and the $\mu\gamma\not\!\!E_T$ sample (points in the right-hand four plots) in a) H_T, the sum of the transverse energies of the lepton, photon, jets and $\not\!\!E_T$; b) the distance in η-ϕ space between the photon and lepton; c) the angular separation in ϕ between the lepton and the missing transverse energy, $\not\!\!E_T$; and d) the invariant mass of the $\ell\gamma$ system. The histograms show the expected SM contributions, including estimated backgrounds from misidentified photons and leptons.

ter response [31] for jets with uncorrected $E_T > 15$ GeV and $\eta < 2.0$, and for muons with $p_T > 20$ GeV.

The variable H_T is defined for each event as the sum of the transverse energies of the leptons, photons, jets, and $\not\!\!E_T$ that pass the above selection criteria.

IV. CONTROL SAMPLES

Because we are looking for processes with small cross sections, and hence small numbers of measured events, we use larger control samples to validate our understanding of the detector performance and to measure efficiencies and backgrounds.

We use $W^{\pm}$ and Z events reconstructed from the same

inclusive lepton datasets as control samples to ensure that the efficiencies for high-p_T electrons and muons are well understood. In addition, the $W^{\pm}$ samples provide the control samples for the understanding of $\not\!\!E_T$. The

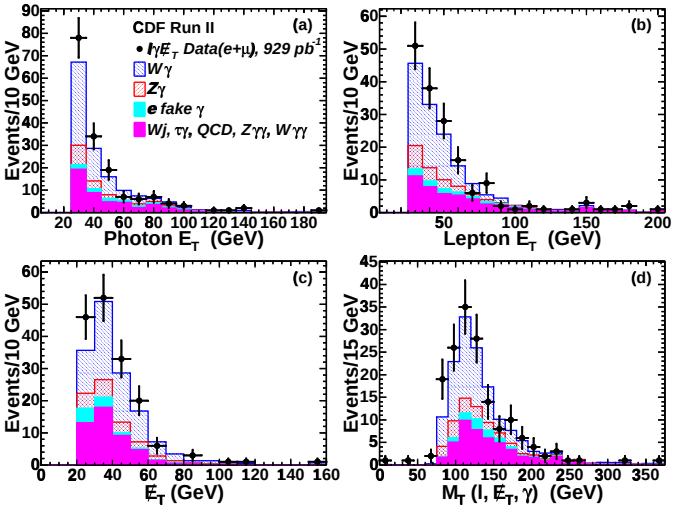

FIG. 4: The distributions for events in the $\ell\gamma\not\!\!E_T$ sample (points) in a) the E_T of the photon; b) the E_T of the lepton (e or μ); c) the missing transverse energy, $\not\!\!E_T$; and d) the transverse mass of the $\ell\gamma\not\!\!E_T$ system. The histograms show the expected SM contributions, including estimated backgrounds from misidentified photons and leptons.

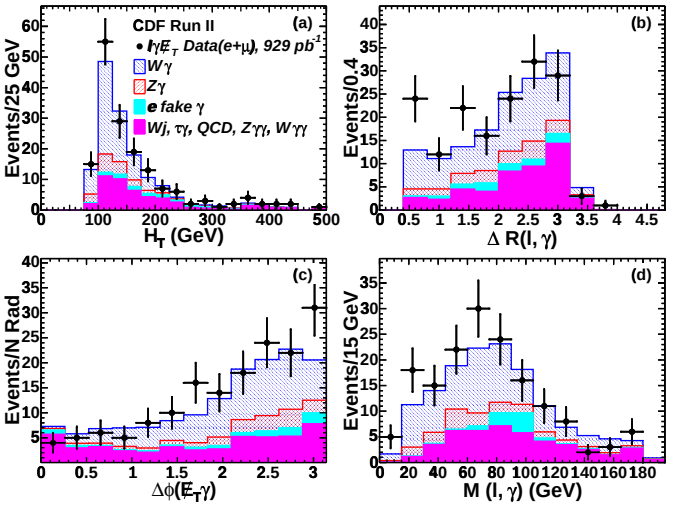

FIG. 5: The distributions for events in the $\ell\gamma\not\!\!E_T$ sample (points) in a) H_T, the sum of the transverse energies of the lepton, photon, jets and $\not\!\!E_T$; b) the distance in η-ϕ space between the photon and lepton; c) the angular separation in ϕ between the lepton and $\not\!\!E_T$; and d) the invariant mass of the $\ell\gamma$ system. The histograms show the expected SM contributions, including estimated backgrounds from misidentified photons and leptons.

selection criteria for the W samples require a tight lepton and $\not\!\!E_T > 25$ GeV. We find 571194 $W \to e\nu$ events and 381727 $W \to \mu\nu$ events. For the Z samples we require two leptons, at least one of which satisfies the tight criteria. We find 30808 $Z \to e^+e^-$ events and 30086 $Z \to \mu^+\mu^-$ events. The photon control sample is constructed from $Z \to e^+e^-$ events in which one of the electrons radiates a high-E_T γ such that the $e\gamma$ invariant mass is within 10 GeV of the Z mass.

V. THE INCLUSIVE $\ell\gamma$+X EVENT SAMPLE

A total of 1678 events, 1479 inclusive $e\gamma$ and 199 inclusive $\mu\gamma$ candidates, pass the $\ell\gamma$ selection criteria. Of the 1479 inclusive $e\gamma$ events, 1130 have the electron and photon within 30° of back-to-back in φ, $\not\!\!E_T < 25$ GeV, and no additional leptons or photons. These are dominated by $Z \to e^+e^-$ decays in which one of the electrons radiates a high-E_T photon while traversing material before entering the COT active volume, leading to the observation of an electron and a photon approximately back-to-back in φ, with an $e\gamma$ invariant mass close to the Z mass.

VI. THE INCLUSIVE $\ell\gamma\not\!\!E_T$ EVENT SAMPLE

The first search we perform is in the $\ell\gamma\not\!\!E_T + X$ subsample, defined by requiring that an event contain $\not\!\!E_T >$ 25 GeV in addition to the γ and "tight" lepton. Of the 1678 $\ell\gamma$ events, 96 $e\gamma\not\!\!E_T$ events and 67 $\mu\gamma\not\!\!E_T$ events pass the $\not\!\!E_T$ requirement.

A. Kinematic Distributions in the Electron and Muon Samples

The muon and electron signatures have different backgrounds and detector resolutions, among other differences. While these are corrected for, it is useful to plot the observed distributions separately before combining them. We show both the individual sample distributions as well as the final combined plot [32].

1. *Distributions in Photon E_T, Lepton E_T, $\not\!\!E_T$, and 3-Body Transverse Mass*

Figure 2 shows the observed distributions in a) the E_T of the photon; b) the E_T of the lepton; c) $\not\!\!E_T$; and d) the transverse mass of the $\ell\gamma\not\!\!E_T$ system, where $\mathrm{M_T} = [(\mathrm{E_T^{\ell}} + \mathrm{E_T^{\gamma}} + \not\!\!\mathrm{E_T})^2 - (\vec{E}_T^{\ell} + \vec{E}_T^{\gamma} + \vec{\not\!\!E}_T)^2]^{1/2}$. The left-hand set of four plots shows the distributions for electrons; the right-hand set shows the distributions for muons.

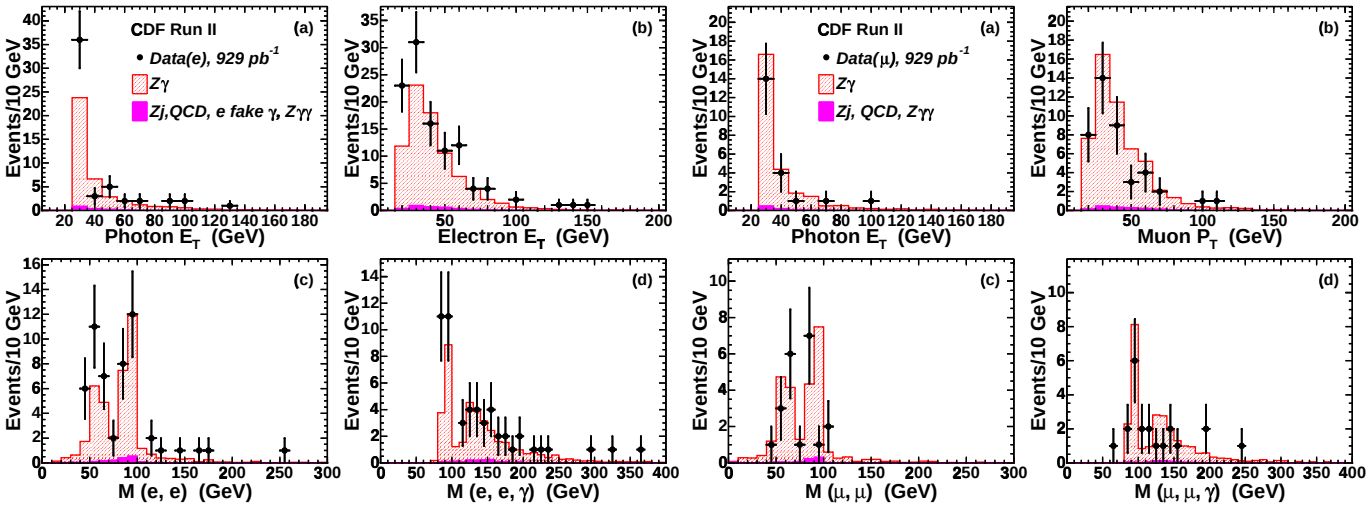

FIG. 6: The distributions for events in the $ee\gamma$ sample (points in the left-hand four plots) and the $\mu\mu\gamma$ sample (points in the right-hand four plots) in a) the E_T of the photon; b) the E_T (p_T) of the electrons (muons) (two entries per event); c) the 2-body mass of the dilepton system; and d) the 3-body mass $M_{\ell\ell\gamma}$. The histograms show the expected SM contributions.

2. *Distributions in H_T, $\Delta\phi_{\ell\gamma}$,$\Delta\phi_{\not\!\!E_T}$, $M_{e\gamma}$*

Figure 3 shows the distributions for the $e\gamma\not\!\!E_T$ sample (left) and $\mu\gamma\not\!\!E_T$ sample (right) in a) H_T, the sum of the transverse energies of the lepton, photon, jets, and $\not\!\!E_T$; b) the distance in η-ϕ space between the photon and lepton; c) the angular separation in ϕ between the lepton and the missing transverse energy, $\not\!\!E_T$; and d) the invariant mass of the $\ell\gamma$ system. The histograms show the expected SM contributions, including estimated backgrounds from misidentified photons and leptons.

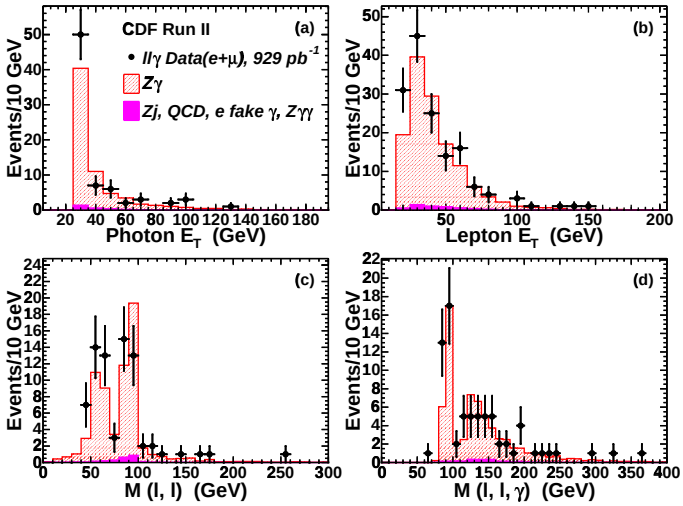

FIG. 7: The distributions for events in the $\ell\ell\gamma$ sample (points) in a) the E_T of the photon; b) the E_T of the leptons (two entries per event); c) the 2-body mass of the dilepton system; and d) the 3-body mass $M_{\ell\ell\gamma}$. The histograms show the expected SM contributions.

The electron and muon kinematic distributions are combined in Fig. 4 and Fig. 5. There is very good agreement with the expected standard model shapes.

VII. THE INCLUSIVE $\ell\ell\gamma$ EVENT SAMPLE

A second search, for the $\ell\ell\gamma + X$ signature, is constructed by requiring another e or μ in addition to the "tight" lepton and the γ.

The $\ell\ell\gamma$ search criteria select 74 events (53 $ee\gamma$ and 21 $\mu\mu\gamma$) of the 1678 $\ell\gamma$ events. No $e\mu\gamma$ events are observed.

3. *Distributions in Photon E_T, Lepton E_T, Dilepton Invariant Mass, and $\ell\ell\gamma$ Mass*

Figure 6 shows the observed distributions in the signature $ee\gamma$ (left-hand plots) and $\mu\mu\gamma$ channels (right-hand plots) for: a) the E_T of the photon; b) the E_T of the electrons; c) the 2-body mass of the dilepton system; and d) the 3-body mass $M_{ee\gamma}$ or $M_{\mu\mu\gamma}$. For the $Z\gamma$ process occurring via initial state radiation, the dilepton invariant mass $M_{\ell\ell}$ distribution is peaked around the Z^0-pole. For the final state radiation, the three body invariant mass $M_{\ell\ell\gamma}$ distribution is peaked about the Z^0-pole.

The combined distributions for electrons and muons are shown in Fig. 7.

4. *Distributions in H_T and $\Delta R_{\ell\gamma}$*

Figure 8 shows the distributions for the $ee\gamma$ sample (left-hand plots) and $\mu\mu\gamma$ sample (right-hand plots) for: a) H_T, the sum of the transverse energies of the electron,

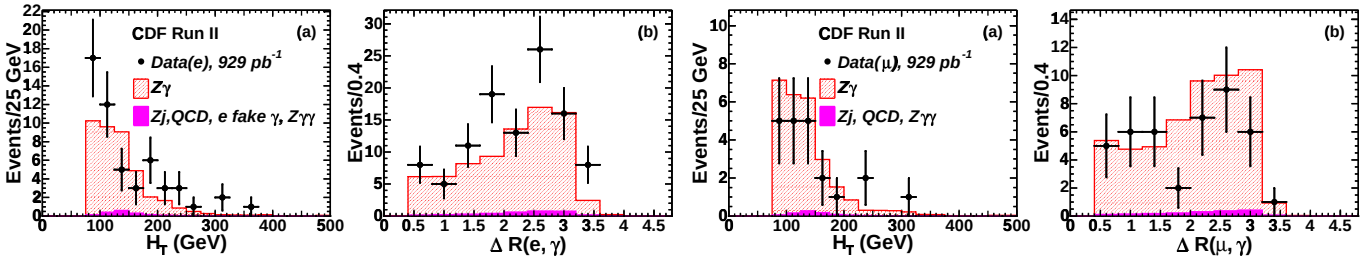

FIG. 8: The distributions for events in the $ee\gamma$ sample (points in the left-hand two plots) and the $\mu\mu\gamma$ sample (points in the right-hand two plots) in a) H_T, the sum of the transverse energies of the lepton, photon, jets and $\not\!\!E_T$; b) the distance in η-ϕ space between the photon and each of the two leptons (two entries per event). The histograms show the expected SM contributions, including estimated backgrounds from misidentified photons and leptons.

photon, jets and $\not\!\!E_T$; b) and the distance in η-ϕ space between the photon and each of the two leptons. The histograms show the expected SM contributions, including estimated backgrounds from misidentified photons and leptons. The distributions for electrons and muons are combined in Fig. 9.

5. *The Distributions in $\not\!\!E_T$*

We do not expect SM events with large $\not\!\!E_T$ in the $\ell\ell\gamma$ sample; the Run I $ee\gamma\gamma\not\!\!E_T$ event was of special interest in the context of supersymmetry [33] due to the large value

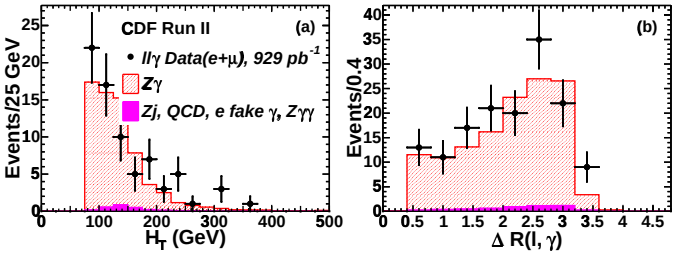

FIG. 9: The distributions for events in the $\ell\ell\gamma$ sample (points) in a) H_T, the sum of the transverse energies of the lepton, photon, jets and $\not\!\!E_T$; b) the distance in η-ϕ space between the photon and each of the two leptons (two entries per event). The histograms show the expected SM contributions, including estimated backgrounds from misidentified photons and leptons.

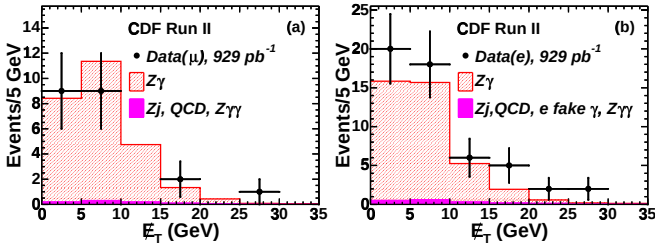

FIG. 10: The distributions in missing transverse energy $\not\!\!E_T$ observed in the inclusive search for a) $\mu\mu\gamma$ events and b) $ee\gamma$ events. The histograms show the expected SM contributions.

of $\not\!\!E_T$ (55 $\pm$ 7 GeV). Figure 10 shows the distributions in $\not\!\!E_T$ for the $\mu\mu\gamma$ and $ee\gamma$ subsamples of the $\ell\ell\gamma$ sample. We observe 3 $\ell\ell\gamma$ events with $\not\!\!E_T > 25$ GeV, compared to an expectation of 0.6 ± 0.1 events.

VIII. SEARCH FOR THE $\ell\gamma\gamma$ SIGNATURE

In some models of new phenomena the decay chain of each of a pair of new heavy particles ends in a photon plus other particles [33]. One such signature that contains two photons and is a subset of the $\ell\gamma+X$ selection is $\ell\gamma\gamma$.

The selection for the $\ell\gamma\gamma$ search starts with a tight lepton and a photon, each with $E_T > 25$ GeV, from the same $\ell\gamma+X$ sample as the $\ell\gamma\not\!\!E_T$ and $\ell\ell\gamma$ searches. An additional photon with $E_T > 25$ GeV, passing the same selection criteria as the first, is then required. We observe no $\ell\gamma\gamma$ events, compared to the expectation of 0.62 ± 0.15.

IX. STANDARD MODEL EXPECTATIONS

A. $W\gamma$, $Z\gamma$, $W\gamma\gamma$, $Z\gamma\gamma$

The dominant SM source of $\ell\gamma$ events is electroweak W and Z/γ^* production along with a γ radiated from one of the charged particles involved in the process [34]. The number of such events is estimated using leading-order (LO) event generators [35–37]. Initial-state radiation is simulated by the PYTHIA Monte Carlo (MC) program [38] tuned to reproduce the underlying event. The generated particles are then passed through a full detector simulation, and these events are then reconstructed with the same code used for the data.

The expected contributions from $W\gamma$ and $Z/\gamma^*+\gamma$ production to the $\ell\gamma\not\!\!E_T$ and $\ell\ell\gamma$ searches are given in Tables I and II, respectively. The expected contributions to the $e\mu\gamma$ search are given in Table IV. A correction for higher-order processes (K-factor) that depends on both the dilepton mass and photon E_T has been applied [39]. In the $\ell\gamma\not\!\!E_T$ signature we expect 71.50 ± 10.01 events from $W\gamma$ and 17.75 ± 3.65 from $Z/\gamma^*+\gamma$. In the $\ell\ell\gamma$ signature, we expect 63.40 ± 7.48 events from $Z/\gamma^*+\gamma$; the

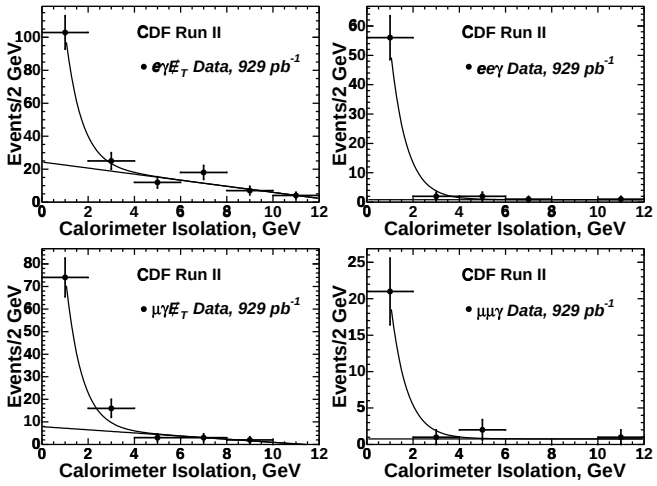

FIG. 11: The method and data used to estimate the number of background events from jets misidentified as photons. For each of the four samples, $e\gamma\not\!\!E_T$ (left top), $ee\gamma$ (right top), $\mu\gamma\not\!\!E_T$ (left bottom), and $\mu\mu\gamma$ (right bottom), the number of events is plotted versus the total (electromagnetic plus hadronic) calorimeter energy, E_T^{Iso}, in a cone in η-ϕ space around the photon. This distribution is then fitted to the shape measured for electrons from $Z \to e^+e^-$ decays plus a linear background.

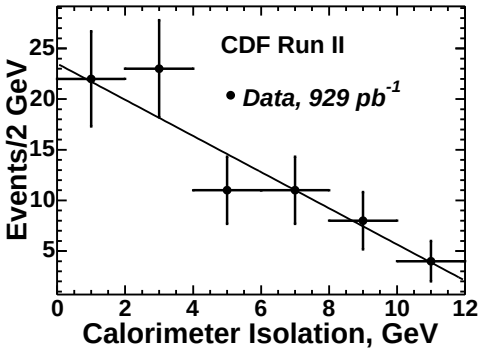

FIG. 12: The distribution in the total calorimeter energy, E_T^{Iso}, in a cone in η-ϕ space around the fake photon candidate. This distribution is then fitted with a linear function.

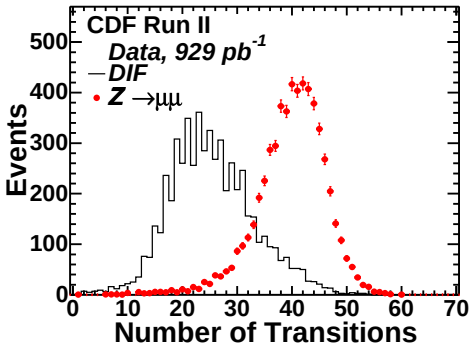

FIG. 13: The method and data used to estimate the number of background muons from low-momentum hadrons decaying in flight. The number of transitions in muons in the $Z \to \mu^+\mu^-$ sample is shown as points. The number of transitions in muons in the sample enriched in hadron decays is shown in the histogram, the so called decay-in-flight ("DIF") sample. The selection criteria for the DIF sample require a tight muon with large impact parameter d_0 >0.2 cm, at least one jet and $\not\!\!E_T$ > 25 GeV.

contribution from $W\gamma$ is negligible. The uncertainties on the SM contributions include those from parton distribution functions (5%), factorization scale (2%), K-factor (3%), a comparison of different MC generators ($\sim$ 5%), and the luminosity (6%).

We have used both MADGRAPH [35] and COMPHEP[37] to simulate the triboson channels $W\gamma\gamma$ and $Z\gamma\gamma$. The expected contributions are small, 0.97±0.12 and 1.14±0.13 events in the $\ell\gamma\not\!\!E_T$ and $\ell\ell\gamma$ signatures, respectively. The expected contributions from $W\gamma\gamma$ and $Z/\gamma^*+\gamma\gamma$ production to the $\ell\gamma\gamma$ search are given in Tables I and III.

B. Backgrounds from Misidentifications

1. *"Fake" Photons*

High p_T photons are copiously created from hadron decays in jets initiated by a scattered quark or gluon. In particular, mesons such as the π^0 or η decay to photons which may satisfy the photon selection criteria. The numbers of lepton-plus-misidentified-jet events expected in the $\ell\gamma\not\!\!E_T$ and $\ell\ell\gamma$ samples are determined by measuring energy in the calorimeter nearby the photon candidate.

For each of the four samples, $e\gamma\not\!\!E_T$, $\mu\gamma\not\!\!E_T$, $ee\gamma$, and $\mu\mu\gamma$, Figure 11 shows the distribution in the total (electromagnetic plus hadronic) calorimeter energy, E_T^{Iso}, in a cone of radius $R = 0.4$ in η-ϕ space around the photon candidate. This distribution is then fitted to the shape measured for electrons from $Z \to e^+e^-$ decays plus a linear background.

To verify the linear behavior of the background we select a sample of "fake photons" by requiring the photon candidate fail the cluster profile criteria. In addition we do not apply the calorimeter and track isolation requirements. The distribution in the total calorimeter energy, E_T^{Iso}, in a cone of radius $R = 0.4$ in η-ϕ space around the fake photon candidate is shown in Fig. 12.

The predicted number of events with jets misidentified as photons is 27.7±6.0 for the $\ell\gamma\not\!\!E_T$ signature and $0.0^{+1.6}_{-0.0}$ for $\ell\ell\gamma$.

For the $\ell\gamma\gamma$ and $e\mu\gamma$ samples, due to the low statistics, the above method cannot be used to find the numbers of background events with a jet mis-identified as a photon. We instead measure the jet E_T spectrum in $\ell\gamma$+jet, ℓ+at least two jets, and $e\mu$+jet samples[40], respectively, and then multiply by the probability of a jet being misidentified as a photon, $P_\gamma^{jet}(E_T)$, which is mea-

TABLE I: A comparison of the numbers of events predicted by the SM and the observations for the $\ell\gamma\not\!\!E_T$ signature. The SM predictions are dominated by $W\gamma$ and $Z\gamma$ production [35–37]. Other contributions come from $W\gamma\gamma$ and $Z\gamma\gamma$, leptonic τ decays, and misidentified leptons, photons, or $\not\!\!E_T$.

Lepton+Photon+$\not\!\!E_T$ Events, $\mathcal{L}$ = 929 pb^{-1}			
SM Source	$e\gamma\not\!\!E_T$	$\mu\gamma\not\!\!E_T$	$(e+\mu)\gamma\not\!\!E_T$
$W^{\pm}\gamma$	41.65 ± 4.84	29.85 ± 5.62	71.50 ± 10.01
$Z/\gamma^* + \gamma$	3.65 ± 1.31	14.10 ± 2.36	17.75 ± 3.65
$W^{\pm}\gamma\gamma$	0.32 ± 0.04	0.18 ± 0.03	0.50 ± 0.06
$Z/\gamma^* + \gamma\gamma$	0.09 ± 0.01	0.38 ± 0.05	0.47 ± 0.06
$t\bar{t}\gamma$	0.88 ± 0.12	0.54 ± 0.08	1.42 ± 0.19
$\ell e\not\!\!E_T$, $e \to \gamma$	9.59 ± 0.76	1.43 ± 0.23	11.02 ± 0.81
$W^{\pm}$+Jet faking γ	21.5 ± 4.8	6.2 ± 3.6	27.7 ± 6.0
$W^{\pm}\gamma, Z/\gamma^* + \gamma \to \tau\gamma$	2.15 ± 0.56	0.76 ± 0.24	2.91 ± 0.65
QCD (Jets faking $\ell + \not\!\!E_T$)	15.0 ± 4.1	$0.0^{+0.1}_{-0.0}$	15.0 ± 4.1
DIF (Decays-In-Flight)	–	2.3 ± 0.7	2.3 ± 0.7
Total SM Prediction	$\mathbf{94.8 \pm 8.1}$	$\mathbf{55.7 \pm 7.1}$	$\mathbf{150.6 \pm 13.0}$
Observed in Data	**96**	**67**	**163**

sured in data samples triggered on jets. The uncertainty on the number of such events is calculated by using the measured jet spectrum and the upper and lower bounds on the E_T-dependent misidentification rate.

The misidentification rate is $P_\gamma^{jet} = (6.5 \pm 3.3) \times 10^{-4}$ for $E_T^\gamma = 25$ GeV, and $(4.0 \pm 4.0) \times 10^{-4}$ for $E_T^\gamma = 50$ GeV [34]. The predicted number of events with jets misidentified as photons is 0.10 ± 0.09 for the $\ell\gamma\gamma$ signature and 0.05 ± 0.01 for $e\mu\gamma$.

The probability that an electron undergoes hard bremsstrahlung and is misidentified as a photon, P_γ^e, is measured from the photon control sample. The number of misidentified $e\gamma$ events divided by twice the number of ee events gives P_γ^e=(1.67 ± 0.07)%. Applying this misidentification rate to electrons in the inclusive lepton samples, we predict that 9.59 ± 0.76 and 0.38 ± 0.11 events pass the selection criteria for the $\ell\gamma\not\!\!E_T$ and $\ell\ell\gamma$ searches, respectively. For the $\ell\gamma\gamma$ search the estimated background is 0.41 ± 0.12 events.

2. *QCD Backgrounds to the $\ell\gamma\not\!\!E_T$ and $\ell\ell\gamma$ Signatures*

We have estimated the background due to events with jets misidentified as $\ell\gamma\not\!\!E_T$ or $\ell\ell\gamma$ signatures by studying the total p_T of tracks in a cone in $\eta - \varphi$ space of radius $R = 0.4$ around the lepton track. We estimate there are 15.0 ± 4.1 and $0.0^{+0.2}_{-0.0}$ events in the $\ell\gamma\not\!\!E_T$ and $\ell\ell\gamma$ signatures, respectively [41].

There is a muon background that we expect escapes the above method. A low-momentum hadron, not in an energetic jet, can decay to a muon forming a "kink" between the hadron and muon trajectories. In this case a high-momentum track may be reconstructed from the initial track segment due to the hadron and the secondary track segment from the muon [42]. The contribution from this background is estimated by identifying tracks consistent with a "kink" in the COT. We count the number of times that, proceeding radially along a COT track, a "hit" in the n+1 layer of sense-wires is on the other side of the fitted track from the hit in the nth layer. Real tracks will have hits distributed on both sides of the fit, and will therefore have many "transitions". A mis-measured track from a 5-GeV K^+ (for example), on the other hand, will consist of two intersecting low-momentum arcs fit by a high momentum track, and will have a small number of transitions [43].

Figure 13 shows the number of transitions in muons in the $Z \to \mu^+\mu^-$ control sample, and in a sample enriched in hadron decays by selecting events with a large $\not\!\!E_T > 25$ GeV, at least one jet and muon that have large impact parameter $d_0 > 0.2$ cm. We estimate that there are 2.3 ± 0.7 and $0.0^{+0.2}_{-0.0}$ events from decay-in-flight in the $\mu\gamma\not\!\!E_T$ and $\mu\mu\gamma$ samples, respectively.

X. RESULTS

The predicted and observed totals for the $\ell\gamma\not\!\!E_T$ and $\ell\ell\gamma$ searches are shown in Tables I and II, respectively. We observe 163 $\ell\gamma\not\!\!E_T$ events, compared to the expectation of 150.6 ± 13.0 events. In the $\ell\ell\gamma$ channel, we observe 74 events, compared to an expectation of 65.1 ± 7.7 events. There is no significant excess in either signature.

The predicted and observed kinematic distributions for the $e\gamma\not\!\!E_T$ and $\mu\gamma\not\!\!E_T$ signatures are compared in Figs. 2 and 3. The corresponding distributions for the $\ell\gamma\not\!\!E_T$ signature (the sum of electrons and muons) are compared in Figs. 4 and 5.

The predicted and observed kinematic distributions for the $ee\gamma$ and $\mu\mu\gamma$ signatures are compared in Figs. 6 and 8. The distributions for the $\ell\ell\gamma$ signature are compared in Figs. 7, 9 and 10. We do find 3 $\ell\ell\gamma$ events with $\not\!\!E_T > 25$ GeV, compared to an expectation of 0.6 ± 0.1

TABLE II: A comparison of the numbers of events predicted by the SM and the observations for the $\ell\ell\gamma$ signature. The SM predictions are dominated by $Z\gamma$ production [35–37]. Other contributions come from $Z\gamma\gamma$, and misidentified leptons, photons, or $\not\!\!E_T$.

Multi-Lepton + Photon Events, $\mathcal{L} = 929$ pb^{-1}			
SM Source	$ee\gamma$	$\mu\mu\gamma$	$(ee+\mu\mu)\gamma$
Z/γ^*	37.85 ± 4.65	25.55 ± 2.88	63.40 ± 7.48
$Z/\gamma^* + \gamma\gamma$	0.72 ± 0.09	0.40 ± 0.05	1.12 ± 0.13
$W^{\pm}\gamma\gamma$	0.016 ± 0.004	$0.0^{+0.001}_{-0.0}$	0.016 ± 0.004
Z/γ^*+Jet faking γ	$0.0^{+1.2}_{-0.0}$	$0.0^{+1.1}_{-0.0}$	$0.0^{+1.6}_{-0.0}$
$\ell\ell e$, $e \to \gamma$	0.38 ± 0.11	0.16 ± 0.07	0.54 ± 0.13
QCD (Jets faking $\ell + \not\!\!E_T$)	$0.0^{+0.2}_{-0.0}$	$0.0^{+0.1}_{-0.0}$	$0.0^{+0.2}_{-0.0}$
DIF (Decays-In-Flight)	–	$0.0^{+0.2}_{-0.0}$	$0.0^{+0.2}_{-0.0}$
Total SM Prediction	$\mathbf{39.0 \pm 4.8}$	$\mathbf{26.1 \pm 3.1}$	$\mathbf{65.1 \pm 7.7}$
Observed in Data	**53**	**21**	**74**

events, corresponding to a likelihood of 2.4%. We do not consider this significant, and there is nothing in these 3 events to indicate they are due to anything other than a fluctuation. We observe no $\ell\ell\gamma$ events with multiple photons and so find no events like the $ee\gamma\gamma\not\!\!E_T$ event of Run I.

The predicted and observed totals for the $\ell\gamma\gamma$ and $e\mu\gamma$ searches are shown in Tables III and IV, respectively. We observe no $\ell\gamma\gamma$ or $e\mu\gamma$ events, compared to the expectation of 0.62 ± 0.15 and 1.0 ± 0.3 events, respectively.

XI. CONCLUSIONS

In Run I, in a sample of 86 pb^{-1} of $p\bar{p}$ collisions at an energy of 1.8 TeV, the CDF experiment observed a single clean event consistent with having a pair of high-E_T electrons, two high-E_T photons, and large $\not\!\!E_T$ [2]. A subsequent search for "cousins" of the $ee\gamma\gamma\not\!\!E_T$ signature in the inclusive signature $\ell\gamma + X$ found 16 events with a SM expectation of 7.6 ± 0.7 events, corresponding in likelihood to a 2.7 σ effect [11, 12].

To test whether something new was really there in either the $\ell\ell\gamma\gamma\not\!\!E_T$ or $\ell\gamma\not\!\!E_T$ signatures, we have repeated the $\ell\gamma + X$ search for inclusive lepton + photon production with the same kinematic requirements as the Run I search, but with an exposure more than 10 times larger, 929 ± 56 pb^{-1}, a higher $p\bar{p}$ collision energy, 1.96 TeV, and the CDF II detector [14]. Using the same selection criteria makes this measurement an *a priori* test, as opposed to the Run I measurement. We find no significant excess in either signature. We conclude that the 2.7 σ effect observed in Run I was a statistical fluctuation.

With respect to the Run I $ee\gamma\gamma\not\!\!E_T$ event, we observe no $\ell\gamma\gamma$ events compared to an expectation of 0.62 ± 0.15 events. The $ee\gamma\gamma\not\!\!E_T$ event thus remains a single event selected *a posteriori* as interesting, but whether it was from SM $WW\gamma\gamma$ production, a rare background, or a new physics process, we cannot determine.

TABLE III: A comparison of the numbers of events predicted by the SM and the observations for the $\ell\gamma\gamma$ signature.

Multi-Photon + Lepton Events, $\mathcal{L} = 929$ pb^{-1}			
SM Source	$e\gamma\gamma$	$\mu\gamma\gamma$	$(e+\mu)\gamma\gamma$
$W^{\pm}\gamma\gamma$	0.021 ± 0.004	0.015 ± 0.003	0.036 ± 0.006
$Z\gamma\gamma$	0.045 ± 0.005	0.038 ± 0.005	0.083 ± 0.007
ℓee, $\ell\gamma e$, $e \to \gamma$	0.41 ± 0.12	$0^{+0.03}_{-0.0}$	0.41 ± 0.12
ℓjj, $\ell\gamma j$, $j \to \gamma$	0.05 ± 0.05	0.05 ± 0.05	0.10 ± 0.09
Total SM Prediction	$\mathbf{0.53 \pm 0.13}$	$\mathbf{0.10 \pm 0.06}$	$\mathbf{0.62 \pm 0.15}$
Observed in Data	**0**	**0**	**0**

TABLE IV: A comparison of the numbers of events predicted by the SM and the observations for the $e\mu\gamma$ signature. The SM predictions are dominated by $Z\gamma$ production [35–37]. Other contributions come from $W\gamma$, $Z\gamma\gamma$, $W\gamma\gamma$, and misidentified leptons, photons, or $\not\!\!E_T$.

eμ + Photon Events, $\mathcal{L} = 929$ pb^{-1}	
SM Source	$e\mu\gamma + X$
$Z/\gamma^* + \gamma$	0.66 ± 0.09
$W^{\pm}\gamma$	$0.10^{+0.18}_{-0.10}$
$Z\gamma\gamma$	0.06 ± 0.01
$W\gamma\gamma$	0.011 ± 0.003
$e\mu j$, $j \to \gamma$	0.05 ± 0.01
$ee\mu$, $e \to \gamma$	0.06 ± 0.05
$W^{\pm}\gamma$, $Z/\gamma^* + \gamma \to \tau\gamma$	$0.09^{+0.18}_{-0.09}$
Total SM Prediction	$\mathbf{1.0 \pm 0.3}$
Observed in Data	**0**

XII. ACKNOWLEDGMENTS

We thank the Fermilab staff and the technical staffs of the participating institutions for their vital contributions. Uli Baur, Alexander Belyaev, Edward Boos, Lev Dudko, Tim Stelzer, and Steve Mrenna were extraordinarily helpful with the SM predictions. This work was supported by the U.S. Department of Energy and National Science Foundation; the Italian Istituto Nazionale di Fisica Nucleare; the Ministry of Education, Culture, Sports, Science and Technology of Japan; the Natural Sciences and Engineering Research Council of Canada; the National Science Council of the Republic of China; the Swiss National Science Foundation; the A.P. Sloan Foundation; the Bundesministerium für Bildung und Forschung, Germany; the Korean Science and Engineering Foundation and the Korean Research Foundation; the Particle Physics and Astronomy Research Council and the Royal Society, UK; the Russian Foundation for Basic Research; the Comisión Interministerial de Ciencia y Tecnología, Spain; in part by the European Community's Human Potential Programme under contract HPRN-CT-2002-00292; and the Academy of Finland.

[1] S.L. Glashow, Nucl. Phys. **22**, 588 (1961); S. Weinberg, Phys. Rev. Lett. **19**, 1264 (1967); A. Salam, Proc. 8th Nobel Symposium, Stockholm, (1979).

[2] F. Abe *et al.* (CDF Collaboration), Phys. Rev. D **59**, 092002 (1999); F. Abe *et al.* (CDF Collaboration), Phys. Rev. Lett. **81**, 1791 (1998); D. Toback, Ph.D. thesis, University of Chicago, 1997.

[3] Transverse momentum and energy are defined as $p_T = p\sin\theta$ and $E_T = E\sin\theta$, respectively. Missing $\mathrm{E_T}$ ($\vec{\not\!\!E}_T$) is defined by $\vec{\not\!\!E}_T = -\sum_i E_T^i \hat{n}_i$, where i is the calorimeter tower number for $|\eta| < 3.6$ (see Ref. [19]), and $\hat{n}_i$ is a unit vector perpendicular to the beam axis and pointing at the i^{th} tower. We correct $\vec{\not\!\!E}_T$ for jets and muons. We define the magnitude $\not\!\!E_T = |\vec{\not\!\!E}_T|$. We use the convention that "momentum" refers to pc and "mass" to mc^2.

[4] For a summary, see: B. C. Allanach *et al.* (Les Houches working group), arXiv:hep-ph/0602198.

[5] D. J. H. Chung, L. L. Everett, G. L. Kane, S. F. King, J. D. Lykken and L. T. Wang, Phys. Rept. **407**, 1 (2005) [arXiv:hep-ph/0312378]. The gravitino is very light, typically a few MeV.

[6] S. P. Martin, arXiv:hep-ph/9709356.

[7] S. Ambrosanio, G. L. Kane, G. D. Kribs, S. P. Martin, and S. Mrenna, Phys. Rev. Lett. **76**, 3498 (1996); G. L. Kane and S. Mrenna, Phys. Rev. Lett. **77**, 3502 (1996); S. Ambrosanio, G. L. Kane, G. D. Kribs, S. P. Martin, and S. Mrenna, Phys. Rev. D **55**, 1372 (1997).

[8] N. Arkani-Hamed, S. Dimopoulos and G. R. Dvali, Phys. Lett. B **429**, 263 (1998) [arXiv:hep-ph/9803315].

[9] D. Acosta *et al.* (CDF Collaboration), Phys. Rev. Lett. **94**, 101802 (2005). A similar search for an excited muon state is given in: A. Abulencia *et al.* (CDF Collaboration), Phys. Rev. Lett. **97**, 191802 (2006) [arXiv:hep-ex/0606043].

[10] See, for example, K. Agashe and G. Servant, JCAP **0502**, 002 (2005) [arXiv:hep-ph/0411254].

[11] D. Acosta *et al.* (CDF Collaboration), Phys. Rev. D **66**, 012004 (2002); hep-ex/0110015.

[12] D. Acosta *et al.* (CDF Collaboration), Phys. Rev. Lett. **89**, 041802 (2002); hep-ex/0202004.

[13] J. Berryhill, Ph.D. thesis, University of Chicago, 2000.

[14] D. Acosta *et al.* (CDF Collaboration), Phys. Rev. D **71**, 032001 (2005).

[15] A. Abulencia *et al.* (CDF Collaboration), Phys. Rev. Lett. **97**, 031801 (2006), hep-ex/0605097; A. Loginov for the CDF Collaboration, Eur. Phys. J. C **46**, s2.21-s2.31 (2006), hep-ex/0604036; A. Loginov, Ph.D thesis, Institute for Theoretical and Experimental Physics, Moscow, Russia, September, 2006.

[16] F. Abe *et al.* (CDF Collaboration), Nucl. Instrum. Methods A **271**, 387 (1988).

[17] A. Affolder *et al.*, Nucl. Instrum. Methods A **526**, 249 (2004).

[18] A. Sill *et al.*, Nucl. Instrum. Methods A **447**, 1 (2000); A. Affolder *et al.*, Nucl. Instrum. Methods A **453**, 84 (2000); C.S. Hill, Nucl. Instrum. Methods A **530**, 1 (2000).

[19] The CDF coordinate system of r, φ, and z is cylindrical, with the z-axis along the proton beam. The pseudorapidity is $\eta = -\ln(\tan(\theta/2))$.

[20] S. Kuhlmann *et al.*, Nucl. Instrum. Methods A **518**, 39 (2004).

[21] The CMU system consists of gas proportional chambers in the region $|\eta| < 0.6$; the CMP system consists of chambers after an additional meter of steel, also for $|\eta| < 0.6$. The CMX chambers cover $0.6 < |\eta| < 1.0$.

[22] A. V. Varganov, Ph.D. Thesis, University of Michigan, 2004; AAT 3137951.

[23] L. Balka *et al.*, Nucl. Instrum. Methods A **267**, 272 (1988).

[24] The fraction of electromagnetic energy allowed to leak into the hadron compartment $\mathrm{E_{had}/E_{em}}$ must be less than $0.055{+}0.00045\times\mathrm{E_{em}}\,(\mathrm{GeV})$ for central electrons, less than 0.05 for electrons in the end-plug calorimeters, less than $\max[0.125,\ 0.055{+}0.00045\times\mathrm{E_{em}}\,(\mathrm{GeV})]$ for photons.

[25] D. Acosta *et al.* (CDF Collaboration), Phys. Rev. D **71**, 051104 (2005); hep-ex/0501023.

[26] The energy deposited in the calorimeter tower traversed by the muon must be less than $2 + max(0, 0.0115 \times (p - 100))$ GeV in the electromagnetic compartment and less than $6 + max(0, 0.028 \times (p - 100))$ GeV in the hadronic compartment.

[27] The muon 'stub' in the muon systems must be within 3, 5, and 6 cm of the extrapolated COT track position, in the CMU, CMP, and CMX muon systems, respectively.

[28] A. Kotwal, H. Gerberich, and C. Hays, Nucl. Instrum. Methods A **480**, 110 (2003).

[29] For tight muons and tight electrons at least 5 hits in each of 3 axial and 3 stereo layers of the COT are required; for loose muons with a matching muon stub this is relaxed to 3 axial and 2 stereo. Loose muons without a matching stub have an additional cut on the χ^2 for the fit to the

track.
[30] Note that this requirement is not a cut on the intrinsic properties of the lepton or photon, but is instead a topological discriminant between those physics processes producing leptons not close to jets (signal) and those with leptons inside jets (presumably background).
[31] A. Bhatti *et al.*, Nucl. Instrum. Methods A **566**, 375 (2006); hep-ex/0510047.
[32] There are no overflows in any of the distributions shown in the figures in this paper.
[33] S. Ambrosanio, G.L. Kane, G.D. Kribs, S.P. Martin, and S. Mrenna, Phys. Rev. D **55**, 1372 (1997); B.C. Allanach, S. Lola, K. Sridhar, Phys. Rev. Lett. **89**, 011801 (2002).
[34] D. Acosta *et al.* (CDF Collaboration), Phys. Rev. Lett. **94**, 041803 (2005).
[35] T. Stelzer and W. F. Long, Comput. Phys. Commun. **81**, 357 (1994); F. Maltoni and T. Stelzer, J. High Energy Phys. **302**, 27 (2003).
[36] U. Baur, T. Han, and J. Ohnemus, Phys. Rev. D **48**, 5140 (1993); J. Ohnemus, Phys. Rev. D **47**, 940 (1993).
[37] E. Boos *et al.* (The COMPHEP Collaboration), Nucl. Instrum. Methods A **534**, 250, (2004); hep-ph/0403113.
[38] T. Sjostrand, Comput. Phys. Commun. **82** (1994) 74; S. Mrenna, Comput. Phys. Commun. **101** (1997) 232.
[39] U. Baur, T. Han and J. Ohnemus, Phys. Rev. D **48**, 5140 (1993); U. Baur, T. Han and J. Ohnemus, Phys. Rev. D **57**, 2823 (1998); hep-ph/9710416; and U. Baur, private communication. The K-factor K_W applied to $W\gamma$ MadGraph MC samples is $K_W = 1.36$ for $M_W \leq 76$ GeV and $K_W = 1.62 + 10^{-5} \times P_T^{\gamma} - 0.386 \times e^{-0.1 \times P_T^{\gamma}}$ for $M_W > 76$ GeV. The K-factor K_Z applied to $Z\gamma$ MadGraph MC samples is $K_Z = 1.36$ for $M_Z \leq 86$ GeV and $K_Z = 1.46 - 0.000728 \times P_T^{\gamma} - 0.125 \times e^{-0.0615 \times P_T^{\gamma}}$ for $M_Z > 86$ GeV.
[40] Following the convention used throughout this paper, these samples are inclusive and are defined by the minimum set of objects required. Any number of additional jets, leptons, or photons, and any value of $\not\!\!E_T$, may also be present.
[41] In each signature the QCD background distribution is derived from the observed data distribution by using the background weight for each observed event; the background level can thus be seen to follow the data in the appropriate figures. The advantage of this procedure (as opposed to just cutting on the track isolation variable) for the low statistics on the tails of the distribution is that one can get some sense of the level of background on the tails of distributions from rare fragmentations of jets that may be topology dependent.
[42] A kaon that decays before the COT volume results in a muon whose momentum is correctly measured; a kaon that decays after the COT is itself correctly measured. These contributions are included in the total background estimate.
[43] We thank A. Paramonov for the method and the code.